

**Studies on the Impact of Long-Term
Correlation on Computer Network
Performance: Part I - Link-layer Modeling**

Hany D. Alsaialy and John A. Silvester

CENG 98-26

**Department of Electrical Engineering - Systems
University of Southern California
Los Angeles, California 90089-2562
(213-740-4579)
December 1998**

Studies on the Impact of Long-Term Correlation on Computer Network Performance: Part I - Link-layer Modeling

Hany D. Alsaialy John A. Silvester
<alsaialy, silvester>@usc.edu

Department of Electrical Engineering-Systems
University of Southern California
Los Angeles, CA 90089-0251

CENG 98-26

Abstract

Several research studies have shown the omnipresence of Long-Range Dependence (LRD) in Local Area Network (LAN) traffic, Wide Area Network (WAN) traffic, and Variable-Bit-Rate (VBR) video traffic [BSTW95], [LTWW94], [LTWW95].

In this paper we present a framework for modeling VBR traffic based on semi-Markov processes. We propose an algorithm based on a simple clustering method to build semi-Markov models for computer network traffic modeling. We introduce our novel mechanism by giving its detailed algorithm, and later analyze its performance by means of simulation. We reveal the efficacy of the proposed method for Long-Range Dependence (LRD) traffic modeling under realistic buffer sizes, and compare the performance of a real computer network Variable-Bit-Rate (VBR) traffic trace with the synthesized traces obtained using our mechanism.

1 Introduction

In recent years, there has been significant attention paid to computer network traffic modeling. This research has increased tremendously since the discovery of Long-Range Dependence (LRD) in real computer network traffic streams [LTWW94]. In [LTWW94] several traces of real computer traffic were collected over a three year period from both Local Area Network (LAN) and Wide Area Network (WAN). When they were analyzed they revealed what is now commonly known as LRD. But what does LRD mean? Simply, and with a high level of abstraction, LRD states that “things that happen far apart cannot be considered independent”. Later, we will give several mathematical characterizations of LRD. After the first results published revealing the omnipresence of LRD in computer network traffic streams, other research studies were done and similar results obtained [GW94]. An example of such a stream is the one from the Star Wars movie encoded using the MPEG standard.

When modeling computer network traffic, it is important to identify the various types of traffic that are found in today’s networks and the quality of service (QOS) expected by the user.

It is clear that the difference in network traffic modeling lies not only on the type of data being transferred (e.g. voice, video, data) or whether the data being transferred is encoded or not, but also on the QOS required by the user. As noted, there is a relationship between the QOS (that concerns the user), and resources that need to be allocated in order to guarantee the

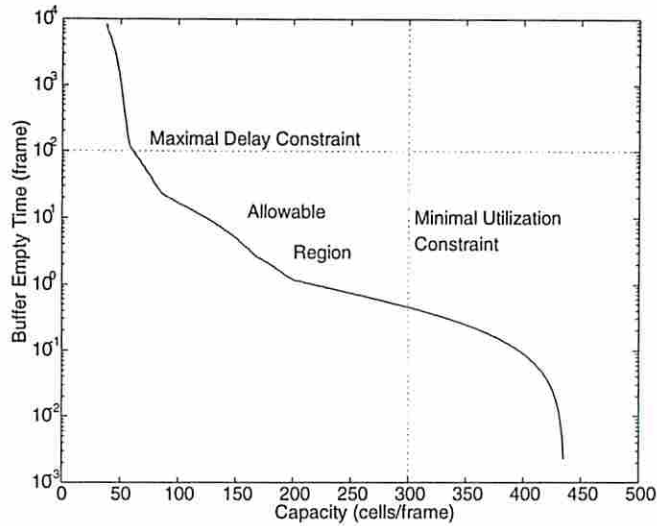


Figure 1: The main fundamental constraints in ATM networks [CG96].

service required (that concerns network management). Unfortunately, there is an inverse relation between QOS and network utilization (e.g. resource allocation), in other words, as utilization increases, overall delays increase which adversely affects the QOS of the users. Both Short-Range Dependence (SRD) and LRD phenomena may impact this utilization/QOS trade-off, so it is important to use traffic models that appropriately represent both factors.

Before proceeding, we emphasize two different aspects of network performance: i) network management, and ii) user requirements. We will later reveal their importance to the concept of traffic modeling. We identify three fundamental constraints [CG96], each constraint affects overall network utilization, or the user performance (i.e. QOS). These three main constraints are:

1. (Maximal) Delay constraint.
2. (Maximal) Loss constraint.
3. (Minimal) Utilization constraint.

Figure 1 shows the constraints graphically¹. It is important to keep these constraints in mind when designing computer network traffic models.

2 Long-Range Dependence in Traffic streams

In the introduction we gave a brief description of LRD, we now present the concept of LRD from a mathematical point of view. There are several ways to describe the concept of LRD, we briefly present some methods, more details can be found in [LTWW94].

Let $X = \{X_i : i \geq 0\}$ be a wide-sense stationary random process. X is LRD if the variance of its aggregate process $X_i^{(m)}$ decreases slowly. This can be checked by the variance-time plot. The

¹Throughout this paper "frame" refers to "frame-time" = $\frac{1}{24}$ second.

variance of the aggregate process $X_i^{(m)}$, is defined as the variance of the number of observations in the new process $X_i^{(m)}$. $X_i^{(m)}$ is obtained by averaging the original process X over non-overlapping blocks of size m ; that is, $X_i^{(m)} = \frac{1}{m}(X_{im-m+1} + \dots + X_{im})$, $i \geq 1$. Mathematically for a process to be LRD we require $\text{var}(X_i^{(m)}) \sim C_1 m^{-D}$ as $m \rightarrow \infty$, $0 < D < 1$. where $D = 2 - 2H$. H is known as the *Hurst* parameter. For a process to be LRD we require $1/2 < H < 1$. Since we have $D = 0$ for $H = 1$, and $D = 1$ for $H = 1/2$, the presence of LRD can be determined by the slope of the variance-time plot; a slope of 0 (i.e. $H = 1$) will indicate strong LRD while a slope of -1 (i.e. $H = 1/2$) indicates the absence of LRD, that is, the process is SRD.

Other conditions that can be used to test a random process for LRD include; testing the autocovariance function $\gamma(k)$, the power spectral density $f(\omega)$, or the mean of its rescaled adjusted range $R(n)/S(n)$. Mathematically, we require $\gamma(k) \sim C_2 k^{-D}$ as $m \rightarrow \infty$, $0 < D < 1$, this can be checked by the empirical autocorrelation function. $f(\omega) \sim C_3 \omega^{-\alpha}$ as $\omega \rightarrow 0$, $0 < \alpha < 1$, this can be checked by the periodogram. Finally, $E[R(n)/S(n)] \sim C_4 n^{-H}$ as $n \rightarrow \infty$, $1/2 < H < 1$, this can be checked by the rescaled adjusted range plot (also called the pox diagram of R/S)[BSTW95]. Note that: $D = 1 - \alpha$. See [BSTW95], [GW94],[LTWW94], [LTWW95] for more details.

In our simulations we will look at the variance-time plot, and other tools we later describe.

3 Basic Clustering Method and Traffic Models Proposed

In this section we introduce the notion of clustering; we first give a generic clustering algorithm, and later introduce the data we wish to cluster.

3.1 How to cluster data

For the time being we introduce the general clustering algorithm, later we will describe the actual data used in our experiments, and see how the clustering method can be used to build the proposed traffic models.

Clustering of data, is performed in the following way:

Algorithm 1 (*Clustering*)

```

1  begin read the first sample  $x_1$ , set  $C_1 \leftarrow x_1$ ,  $n_1 \leftarrow 1$ , and initialize  $Threshold_1$ 2
2  do read the next sample  $x_i$ 
3      do for all clusters  $j$  (with centers  $C_j$ )
4          if there exist a distance,  $d_{ij}$ , from  $x_i$  to  $C_j$  less than the threshold of cluster  $j$ ,
that is;
```

$$d_{ij} = \|x_i - C_j\| < Threshold_j$$

```

5          then select cluster  $j$  having the smallest  $d_{ij}$ 
6      end for
7      if cluster  $j$  (steps 4, 5) is found then
8          update the center of cluster  $j$  by:
```

$$C_j \leftarrow \frac{1}{n_j + 1} \{n_j C_j + x_i\}$$

²A description of the method we use to calculate the threshold is given in section 4.

where $n_j =$ total number of samples in cluster j before adding x_i .

```

9           update  $n_j \leftarrow n_j + 1$ 
10          update  $Threshold_j$ 
11          else form a new cluster as performed in 1
12  until end of stream (or for a reasonable time enough to characterize traffic)
13  end

```

In our experiments we used a stream of VBR video traffic, and converted the stream representing bits/frame to 53 byte ATM cells/frame. We left the measurement rate of 24 frames/sec unchanged. Hence, clustering is performed per-frame. The stream of the full-length Star Wars movie used was originally coded using the MPEG standard measured at frame resolution. Since this known stream resembles real VBR traffic, we choose it to verify the efficacy of the proposed model. Note that this stream is bursty and exhibits LRD as will be shown later.

3.2 Clustering method and Markov Modeling

In this section we describe the method we use to build a pure Markovian model based on the clusters obtained by the algorithm just described.

The data stream represents a sequence of random events, we will therefore specify the analogy of the clustering method to a Discrete-Time Markov Process (DTMP). As part of the clustering process described above, we also maintain the cluster transition history by the matrix T which specifies the number of transitions t_{ij} from cluster i to cluster $j \forall ij$.

The analogy with the DTMP is now clear and easy to formalize. The mapping is done as follows:

- The number of states of the DTMP \longleftrightarrow Number of clusters.
- The average input rate generated in state $i \longleftrightarrow$ Final location of the cluster center C_i .
- The transition probabilities P_{ij} between states $i, j \longleftrightarrow \frac{t_{ij}}{\sum_j t_{ij}} \forall ij$.

Throughout this paper, we will use the terms cluster and state (i.e. state of the Markov or semi-Markov chain) interchangeably.

3.3 Clustering Method and Semi-Markov Modeling

We are now ready to define the steps required to build a Semi-Markov Process (SMP) using the clustering method. We would like to mention that a SMP is not Markovian, in other words, a SMP may or may not be SRD depending on the holding-time in each state, for more details see [Nel95]. A SMP is a generalization of a Markov chain. In such a process we include a pdf to specify the state holding time in each state. Note that if the state holding time follows the geometric or exponential distribution, we would then have a Markov chain. Any other pdf yields to a SMP. In this study, we use holding times distributed according to a Pareto distribution (other holding time distributions could be as well used).

In order to model the holding time H_j for any state j of the semi-Markov chain, we need a sequence of random events representing these holding times. Let $x_{i,j}$ be the random variable

counting the number of $j \rightarrow j$ transitions in a single visit to state j , and m_j be the number of visits to state j observed during the trace, in other words, define $\{X_{m_j,j}\} = x_{1,j}, \dots, x_{m_j,j}$.

To estimate the parameters of a pareto pdf defining the holding-time of state j of our SMP, given $\{X_{m_j,j}\}$, we use the method of maximum likelihood.

The pareto pdf is defined as follows [AFT98]:

$$f(x | \alpha_j, k_j) = \alpha_j k_j^{\alpha_j} x^{-(\alpha_j+1)} \quad \alpha_j, k_j > 0, x \geq k_j \quad (1)$$

where α_j, k_j are the pareto parameters and the subscript j refers to cluster j .

Hence, the likelihood of α_j is:

$$lik(\alpha_j) = \prod_{i=1}^{m_j} f(x_{i,j} | \alpha_j, k_j) \quad (2)$$

and the log-likelihood of α_j is:

$$l(\alpha_j) = \sum_{i=1}^{m_j} \log f(x_{i,j} | \alpha_j, k_j) \quad (3)$$

solving $\frac{\partial}{\partial \alpha_j} l(\alpha_j) = 0$ for α_j we get:

$$\hat{\alpha}_{jMLE} = \frac{m_j}{\sum_{i=1}^{m_j} \log x_{i,j} + m_j \log \tilde{k}_j} \quad \forall j \quad (4)$$

where \tilde{k}_j is an estimate of k_j that can be found solving for k_j numerically using Newton's method [PVT92].

We adjust the transition probabilities P_{ij} to eliminate the self loops by:

$$P_{ij} = \begin{cases} \frac{P_{ij}}{(1-P_{ii})} & \forall i \neq j \\ 0 & \forall i = j \end{cases} \quad (5)$$

The SMP described operates in the following fashion:

1. After entering state i , find the holding time H_i that the process spends in state i before moving to the next state j .
2. Select the next state $j \neq i$ where the transition is to be made.

This is the simplest definition for operating a SMP. In our simulations we used this definition, however, we would like to describe another that requires further investigation:

1. After entering state i , select the next state $j \neq i$ where the transition is to be made.
2. Find the holding time $H_{i,j}$ that the process will spend state i before moving to the next state j (where $H_{i,j}$ is defined as the holding time in state i given that the next state is j).

In this definition, the state holding time depends on the next state transition, in other words, several pdfs define the holding time in a given state. Intuitively, we believe this approach would yields better modeling results.

4 Simulation Results

We use the algorithms described in section 3.1 to build both DTMPs and SMPs by using the VBR video stream from the Star Wars movie, and analyze our results by simulation. We compare several aspects of the original and model generated streams, including, Cell-Loss Rate (CLR) under different network scenarios. We will also compare the behavior of the streams by the Leaky-Bucket Contour plot (LBC) [LNR94]. For the LBC plot method, there are several regions of interest as described in [CG96] see Figure 2. The three main regions are: i) LRD dominant region, ii) SRD dominant region, and iii) Marginal distribution dominant region. Notice that in the clustering method, we produce a processed stream creating a smoothed version of the original. The resulting stream will vary in number of clusters depending on the threshold size of the clusters.

The threshold of a given cluster can be fixed (e.g. Parzen-window method), or made sensitive to the location of the cluster (e.g. k-nearest-neighbor method), for more details see [DH73]. In our experiments we use the latter approach³ by setting the threshold as: $Threshold_j \leftarrow \text{Min}[A + (\frac{B}{100} * C_j), thresh_{\text{max}}]$, where A , B , and $thresh_{\text{max}}$ are set before each simulation run. C_j is the center of cluster j . Since the threshold is set according to the cluster center, we obtained larger thresholds for higher values of C_j ; this helped compensate the larger variability for the higher levels. In our experiments we adjusted $A \approx [5, 15]$, $B \approx [10, 20]$, and $thresh_{\text{max}} \approx 90$. From several simulation runs we found that approximately eight clusters gave good results to characterize the original stream. We later show the similarity of the processed stream compared to the original one, and show that the only difference is in the marginal distribution. In other words, both the original and the smoothed stream are similar in terms of LRD and SRD as the LBC plot will verify. The use of eight quantized levels (clusters in our case) to provide an accurate representation of the stream agree with results reported in [SS93].

4.1 Matching Mean, Variance, and CLR

Table 1 summarizes some statistical results from our experiments.

Trace	Samples	Mean	Peak/Mean Ratio	Variance	States
MPEG stream	174136	36.289	12.015	1835.554	353
Processed stream	174136	35.914	11.305	1836.113	8
DTMP stream	174136	35.725	11.756	1815.807	7-12
SMP stream	174136	26.124	15.962	1225.562	7-12

Table 1: Statistics of the real and synthesized data traces.

The 353 states (or quantized levels) resulted from converting the original stream to ATM cells. In addition, the range in the number of states for the DTMP and SMP stream is due to the fact that several experiments were conducted each with slightly different cluster size. We would also like to mention that we used a deterministic process while in the DTMP/SMP state. We can, however, observe that both a deterministic and a Poisson process would produce similar

³Informally speaking, our approach is an intermediate between the two methods since we adjust the size of the threshold during training. This is known as the "Relaxation method". See [DH73].

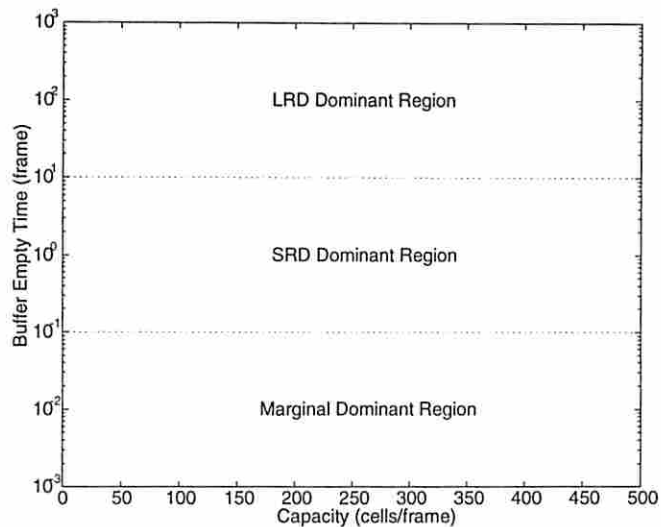


Figure 2: Dominant regions for the three main components of a trace [CG95].

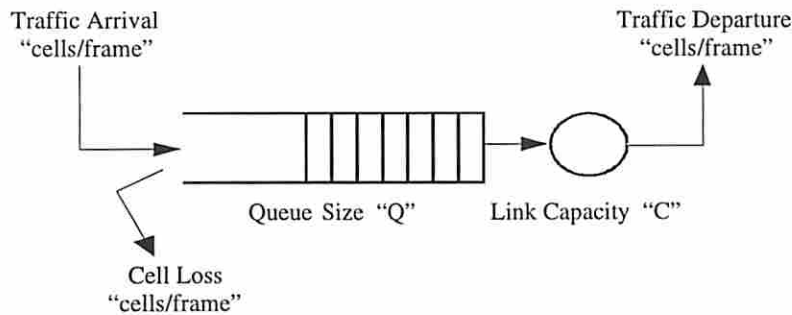


Figure 3: A single queue single server system.

results by comparing the original and processed stream. We observe that the performance impact (e.g. Cell-Loss Rates CLR) is due to: a) number of states, b) transition probabilities P_{ij} , and c) holding-times H_j . The high-frequency component, on the other hand, has only a marginal impact.

We can see from Table 1 that the simple statistics from the DTMP closely matched the average statistics from the original stream. However, we need to investigate the behavior of the streams since we still have no indication of the correlation structure. We further analyze the streams by comparing CLR for different buffer sizes and capacity values, to compare the effects of Long-Range Dependence (LRD) and Short-Range Dependence (SRD). Figures 4, 5, and 6 show the CLR obtained in our simulation. We applied all four streams to a simple FCFS single queue single server system, see Figure 3.

In Figure 4 we used a small buffer size for the wide range of capacity allocation (Maximum Queueing Delay (MQD) ≈ 4.5 – 45 ms), all streams seem to match the behavior of the original stream well due to: a) the effect of SRD is pronounced; or b) we see little effect from LRD. There-

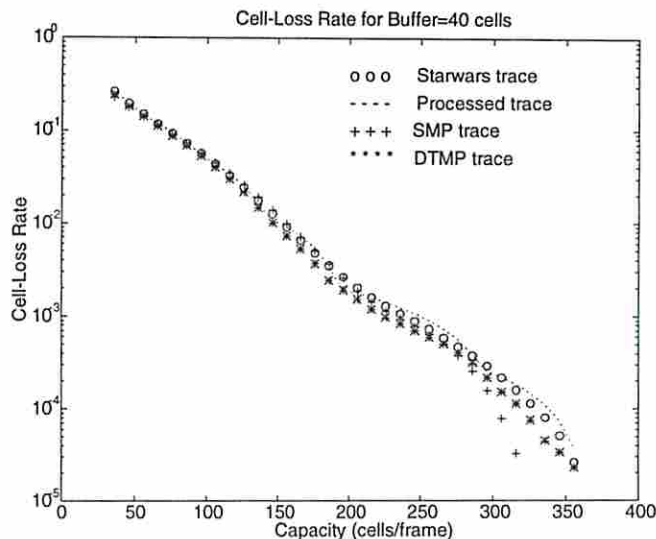


Figure 4: Effect of short-range dependence is pronounced with small buffer size.

fore a well designed SRD Markovian model gave good results under these operational conditions (i.e. relatively small buffer).

In Figure 5, we fixed the link capacity to 60 cells/frame ($\approx 600\text{Kbps}$) and showed results over a wide range of buffer sizes ($\text{MQD} \approx 7\text{--}350\text{ms}$). As the buffer size increases, the effect of LRD become more pronounced making the pure DTMP fail to model the original stream. On the other hand, the SMP model gives better results as expected. We reemphasize the importance of realistic buffer sizes used in simulation due to the QOS expected by the users since as we know, buffer sizes are finite and often small in a real life computer network. More results showing the dominant effect of short-term correlation on CLR can be found in [RE96]. We see, therefore, the efficacy of the proposed semi-Markovian model for VBR traffic modeling.

To validate our results we conducted additional experiments for realistic values of buffer sizes and link capacities. Figure 6 shows results obtained using a link capacity of 250 cells/frame ($\approx 2.5\text{Mbps}$) and ranges from 10 to 120 cell buffers ($\text{MQD} \approx 2\text{--}20\text{ms}$). We can clearly see the good match from the SMP model.

4.2 LBC and VT plots

To fully investigate the behavior of the proposed model we present results obtained by the Leaky-Bucket Contour plot (LBC) [LNR94], as well as a variance-time plot for all our streams.

Figures 7 and 8 show additional results obtained analyzing our four streams of real and synthesized data. In the LBC plot of Figure 7, we assumed the buffer to be infinite (i.e. $\text{CLR}=0$) and the simulation records the maximum buffer occupancy for a range of link capacities; as in [CG96] we plot capacity versus the buffer-empty-time (T) which was found by $T = B/C$, in other words T is simply the MQD measured in frame time (i.e. $\text{MQD} = T/24$ in our case). Figure 7 shows that all streams are matching in part of the SRD dominant region, however, the DTMP - being a pure Markovian process - failed, as expected, to match the original stream in the LRD dominant region. The SMP with non-memoryless state holding times gave better results and

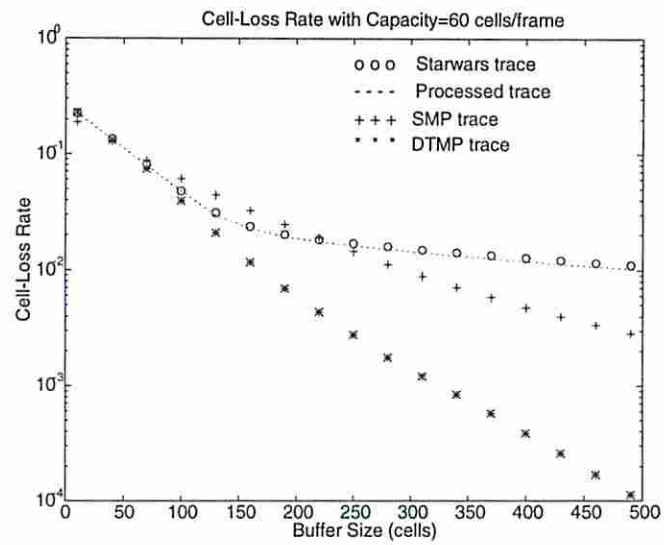


Figure 5: Effect of long-range dependence is pronounced as buffer size increase.

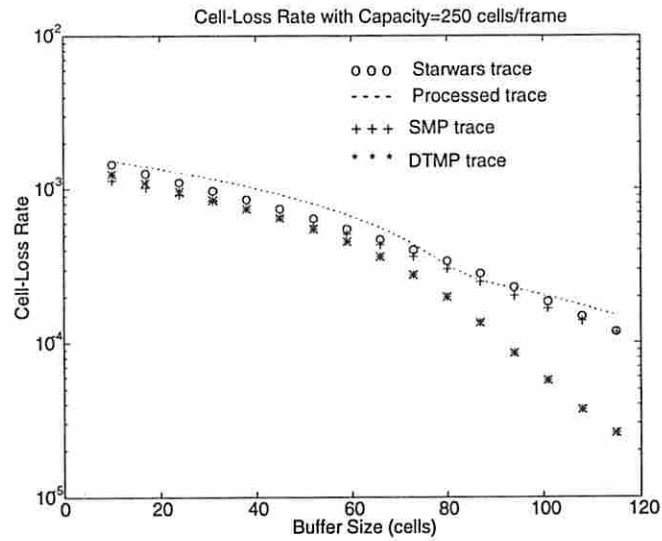


Figure 6: The semi-Markov process matches well under realistic operational scenarios.

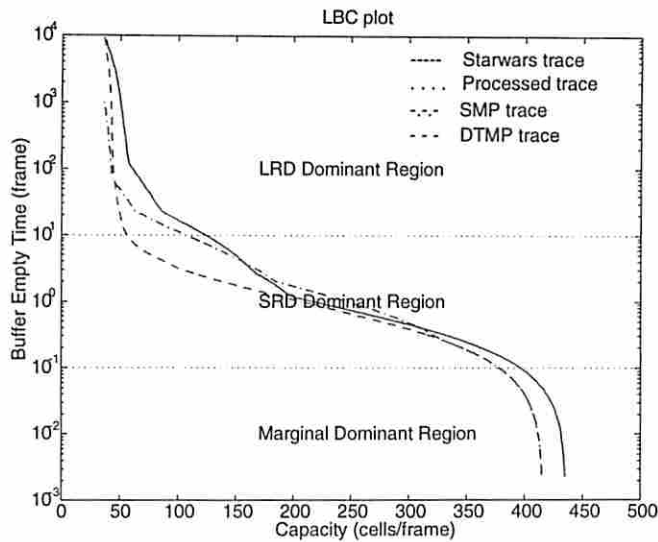


Figure 7: The leaky-bucket contour plot for the four traces.

appears to match some of the correlation structure of the original stream. It is important to remember, however, that the maximal delay and minimal unitization constraints found in real life networks restrict the allowable region for capacity allocation and buffer sizes. As shown in Figure 7, the lower and upper bounds separating the three regions is equivalent to a $MQD \approx 4.167\text{ms}$ and 416.67ms , respectively. We believe, therefore, that the proposed semi-Markov model mimics well the behavior of a real VBR traffic stream under realistic operational scenarios.

Figure 8 shows that the SMP is in fact more bursty in nature than its counterpart Markovian model, we can see that the stream generated by the SMP captured more of the correlation of the original stream. The DTMP, being inherently SRD, quickly loses its correlation as revealed by a slope of -1 (i.e. $H = .5$).

Finally, Figures 9 and 10 depict the actual traces. In Figure 9 we show a small segment of the original and processed trace showing the eight quantized levels. In Figure 10, we show the original, DTMP and SMP trace plotted at different time scales. It is clear that both the SMP and Star Wars trace appear to be more bursty and much more similar compared to the trace generated by the DTMP.

5 Conclusion

From results obtained by simulation, we conclude that the proposed clustering method enabled us to create accurate models for Variable-Bit-Rate (VBR) traffic modeling in computer networks. We used a similar algorithm to build semi-Markovian models and found it to be simple and efficient. Results showed that under realistic operational network scenarios, the impact of Long-Range Dependence (LRD) to determine the Cell-Loss-Rate (CLR) is not of practical importance. We showed that the use of well designed semi-Markovian models can give satisfactory results for computer network traffic modeling and performance evaluation.

We believe that there are still several issues that requires further investigation. Among those

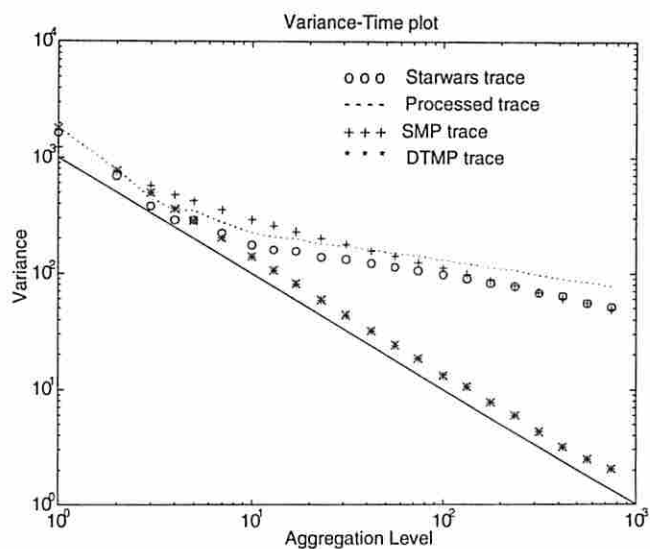


Figure 8: The variance-time plot for the four traces.

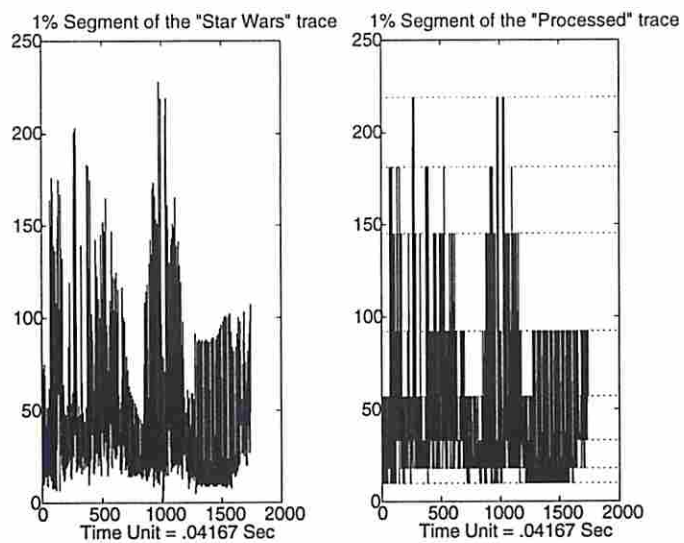


Figure 9: The eight quantized levels of the processed trace.

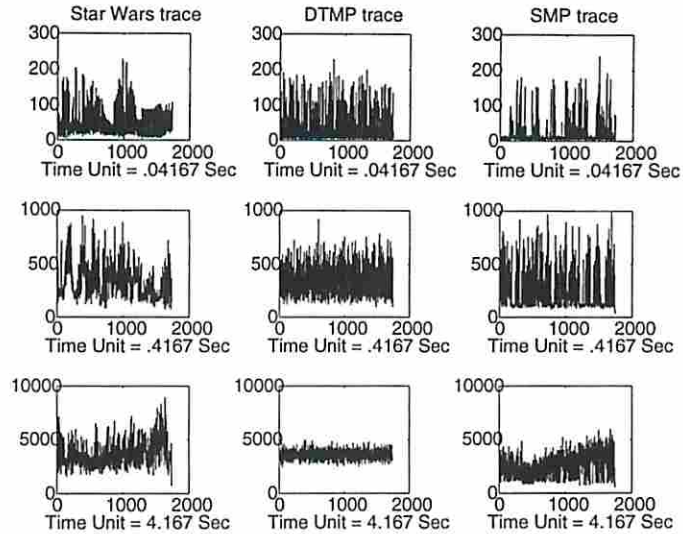


Figure 10: The three data traces shown at different levels of aggregation (Note: a Poisson process was used in the DTMP and SMP state).

are how to formalize an efficient way to define the cluster sizes for best matching a given stream. We would also like to propose the use of different pdfs for state holding times, to see their goodness of fit by means of statistical tools such as the Quantile-Quantile plot [LK91]. We also propose using the data obtained by the clustering method to directly specify an empirical distribution for the modeling of state holding times. As described in Section 3.3, we propose the use of conditional probability for modeling state holding times.

We would also like to mention the possibility of utilizing the proposed clustering method with the Hidden Markov Models (HMM) described in [RJ93]. We propose the use of the clustering method to identify the number of states in the Markov chain and corresponding average rate for each state, and then use the theory of HMM to find the transition probabilities.

Acknowledgement

The first author would like to acknowledge the support of the Institute of Public Administration (IPA), Riyadh, Saudi Arabia.

References

- [AFT98] R. J. Adler, R. E. Feldman, M. S. Taquq, "A Practical Guide to Heavy Tails," Birkhauser, pp. 3-25, 1998.
- [BSTW95] J. Beran, R. Sherman, M. S. Taquq, and W. Willinger, "Long-Range Dependence in Variable-Bit-Rate Video Traffic," IEEE Trans. Commun., vol. 43, no. 2/3/4, pp. 1566-1579, Feb./March/April 1995.

- [CG96] C.-H. Chou and E. Geraniotis, "Performance Prediction and Resource Allocation for Long-Range Dependent Traffic in ATM Networks," Proc. of the 30th Annual Conference on Information Sciences and Systems, pp.198-204, March 1996.
- [DH73] R. O. Duda and P. E. Hart, "Pattern Classification and Scene Analysis," John Wiley & Sons, 1973.
- [GW94] M. Garrett and W. Willinger, "Analysis, Modeling and Generation of Self-Similar VBR Video Traffic," Proc. ACM SIGCOM '94, pp. 269-280, Sep. 1994.
- [LK91] A. M. Law and W. D. Kelton, "Simulation Modeling and Analysis," Second Edition, McGraw-Hill, pp. 375-379, 1991.
- [LNR94] D. M. Lucatoni, M. F. Neuts, and A. R. Reibman, "Methods for Performance Evaluation of VBR Video Traffic Models," IEEE/ACM Trans Networking, vol. 2, no. 2, pp. 176-180, April 1994.
- [LTWW94] W. E. Leland, M. S. Taqqu, W. Willinger, and D. V. Wilson, "On the Self-Similar Nature of Ethernet Traffic (Extended Version)," IEEE/ACM Trans. Networking, vol. 2, no. 1, pp.1-15, Feb. 1994.
- [LTWW95] W. E. Leland, M. S. Taqqu, W. Willinger, and D. V. Wilson, "Self-Similarity in High-Speed Packet Traffic: Analysis and Modeling of Ethernet Traffic Measurements," Statistical Science, vol. 10, no. 1. pp. 67-85, 1995.
- [Nel95] R. Nelson, "Probability, Stochastic Processes, and Queueing Theory," Springer-Verlag, pp. 352-356, 1995.
- [PVTf92] W. H. Press, W. T. Vetterling, S. A. Teukolsky, B. P. Flannery, "Numerical Recipes in C," Second Edition, Cambridge University Press, 1992.
- [RE96] B. K. Ryu and A. Elwalid, "The importance of Long-Range Dependence of VBR video traffic in ATM traffic engineering: Myths and Realities," In Proc. ACM SIGCOMM, San Francisco, CA, 1996.
- [RJ93] L. Rabiner and B. H. Juang, "Fundamentals of Speech Recognition," Prentice Hall, 1993.
- [SS93] P. Skelly and M. Schwartz, "A Histogram-Based Model for Video Traffic Behavior in an ATM Multiplexer," IEEE/ACM Trans. Networking, vol. 1, no. 4, pp. 446-459, Aug. 1993.